



Contents lists available at ScienceDirect

Journal of King Saud University – Science

journal homepage: www.sciencedirect.com

Original article

Green synthesis of silver nanoparticles by employing the *Allium fistulosum*, *Tabernaemontana divaricate* and *Basella alba* leaf extracts for antimicrobial applications

S. Vinodhini ^{a,*}, B. Scholastica Mary Vithiya ^{a,*}, T. Augustine Arul Prasad ^b^a Department of Chemistry, Auxilium College (Affiliated to Thiruvalluvar University, Serkkadu, Vellore - 632115), Vellore - 632006, Tamil Nadu, India^b Department of Chemistry, Dwarakadoss Goverdhanoss Vaishnav College (Affiliated to University of Madras), Chennai - 600106, Tamil Nadu, India

ARTICLE INFO

Article history:

Received 1 January 2022

Revised 20 February 2022

Accepted 28 February 2022

Available online 4 March 2022

Keywords:

Anti-diabetic

Catalytic

Photocatalytic

Antibacterial

Antifungal

Antioxidant *Allium fistulosum**Tabernaemontana divaricate**Basella alba*

Silver nanoparticles

ABSTRACT

Nanoparticles produced from biological sources are gaining a lot of attention these days, and they have a wide spectrum of uses. The fact that it is both environmentally benign is the key reason for its widespread popularity. Our current study uses a green approach to describe the biological production and characterisation of silver nanoparticles made from a conventional leaf extract. The antibacterial and antidiabetic performance of silver nanoparticles prepared with plant extracts such as *Tabernaemontana divaricate*, *Basella alba*, and *Allium fistulosum* is also assessed in this study. Scanning Electron Microscopy (SEM), and Transmission Electron Microscope (TEM) was utilized to characterise the shape and morphology of produced silver nanoparticles. Silver nanoparticles with sizes of 40 nm, 50 nm and 57 nm were observed to have a solid block-like, rod-like structure. AgNPs show bactericidal action towards both gram-positive and -negative microbes, according to in vitro investigations. Both antidiabetic and antioxidant activity suggest that silver nanoparticle has good ability to inhibit enzymes so it could act as alternative for the conventional drug.

© 2022 The Author(s). Published by Elsevier B.V. on behalf of King Saud University. This is an open access article under the CC BY-NC-ND license (<http://creativecommons.org/licenses/by-nc-nd/4.0/>).

1. Introduction

Metallic nanoparticles (NPs) were of major attention due to its exceptional physico-chemical properties and possible photocatalytic and wastewater treatment benefits (George et al., 2022; Maria Magdalane et al., 2018; Panimalar et al., 2022; Panimalar et al., 2022; Kasinathan et al., 2016). Metallic nanoparticles (MNPs) have distinct properties that are determined by the ways of fabrication and the composition of the precursors which is effect of biological and metal oxide nanoparticles (Venkatesh et al., 2018; Simbine et al., 2019; Aziz et al., 2016; Mahmoud et al., 2016; Elbeshehy et al., 2015). Physical methods for preparing AgNPs have been tried, however they are not cost-effective, waste more energy,

and require the use of specialised instruments. However, because of toxicity issues, they have limited biological applicability. External stabilisers, some of which are hazardous, are routinely used to improve their stability. The use of biological resources to produce nanoparticles, particularly plants, can eradicate the toxic issue (Mani et al., 2021; Anand et al., 2017; Mani et al., 2021; Mani et al., 2021). Floras were widely available, non-toxic, and simple to manage. Plants also have phytochemicals, might be reducing and capping substances, making the production method simple. Silver (Ag) NPs have gained a lot of attention among all the metallic nanoparticles (Oves et al., 2018; Manikandan et al., 2017). Chemical-based reduction, micro-emulsions, radiation, hybrid-based approaches, photo-chemical reduction and sono-electrochemical, microwave-based systems, and now a green production route have all been developed for the production of AgNPs (Yaqoob et al., 2020; Syafiuddin et al., 2017; Loo et al., 2018; Sanchooli et al., 2018).

However, despite the fact that some of these physiochemical procedures are long-lasting and technically viable, their usage on a broad scale is limited owing to its usage of dangerous chemicals, higher costs, higher energy and time requirements, and strain in wastage purification through photocatalysis technique (Mangala

* Corresponding authors.

E-mail addresses: vinodhinishanjeevee@gmail.com (S. Vinodhini), scho-12005@auxiliumcollege.edu.in (B. Scholastica Mary Vithiya).

Peer review under responsibility of King Saud University.



Production and hosting by Elsevier

<https://doi.org/10.1016/j.jksus.2022.101939>

1018-3647/© 2022 The Author(s). Published by Elsevier B.V. on behalf of King Saud University.

This is an open access article under the CC BY-NC-ND license (<http://creativecommons.org/licenses/by-nc-nd/4.0/>).

Nagasundari et al., 2021; Kayalvizhi et al., 2022; Perumal et al., 2022; Alhaji et al., 2019; Amanulla et al., 2021). As a result, there was an improving claim for cost-effective, ecologically friendly, and green nanosilver manufacturing pathways that utilize non-toxin chemicals. Green production of AgNPs employing a variety of microbes, plants, and algae, on the other hand, is a natural, biocompatible, and ecologically friendly process (Rajeshkumar and Malarkodi, 2014; Bakht Dalir et al., 2020; Yadi et al., 2018). Plant-based materials may be extra advantageous for nanosilver production than microbial and chemical approaches since they pose no risk of microbial and harmful chemical infection, need lesser energy, have broader consequences, and are easier to utilise. Furthermore, the inclusion of functional substances like phenol, ketones, aldehydes, and so on in the green production of AgNPs based on a plant-based extract mode of actions improves metal ions. AgNPs were produced using a number of organic plants, including *Emblica ffcinalis* fruit extract, Citrus limon leaves extract, green tea – *Camellia sinensis*. *Coffea Arabica* and neem; *Azadirachta indica*; *Acalypha indica*, *Aloe vera* flora extract; latex of *Jatropha gossypifolia*; root extract of *Morinda citrifolia*; *Phoenix dactylifera*, in-florescence of *Mangifera indica* (Nakhjavani et al., 2017; Dhand et al., 2016; Tippyawat et al., 2016; Tippyawat et al., 2016; Rai et al., 2014; Kalaimagal, 2019).

Silver nanoparticles were synthesised using medicinal herbs such as *Tabernaemontana divaricate*, *Basella alba*, and *Allium fistulosum* in this study. Pinwheel flower, *Tabernaemontana divaricata*, belongs to the Apocynaceae family and is a wonderfully shaped evergreen shrub that blooms in spring. Plant extract has antinociceptive, antioxidant, anti-inflammatory, and reversible acetylcholinesterase inhibitory properties, according to studies (Ahmad et al., 2019; Rafique et al., 2017; Masum et al., 2019; Chang et al., 2016; Zuo et al., 2018). *Basella alba*, sometimes known as Indian Spinach, was a fastest-growing perennial vine natural to tropical Asia. It is said to have originated in India or Indonesia and is exceptionally heat tolerant. It has thick, semi-succulent leaves that are heart-like and it has a moderate flavour and mucilaginous texture. It has antinociceptive, antioxidant, and antibacterial properties, and it's also used to treat diarrhoea (Mani et al., 2021; Mani et al., 2021; Yaqoob et al., 2020; Loo et al., 2018). *A. fistulosum* is a traditional medicine that is considered a rich source of nutrients. Several research have revealed the anti-oxidant; antimicrobial; anticancer; antihypercholesterolemic; anti-obesity; and anti-inflammatory activity of *A. fistulosum* for human health. *A. fistulosum's* active chemicals help it perform a variety of biological functions (Zhao et al., 2021; Labh et al., 2019; Zafer et al., 2021). The anti-oxidant size of *A. fistulosum*, for example, is closely associated by its total phenolic composition, while allicin is responsible for its antibacterial activity. Because of the active components contained in most plants, they exhibit a wide spectrum of activities. As a result, the goal of our study was to look at the biological nature of Ag NPs made from three distinct extracts (Zhao et al., 2021; Akintelu and Folorunso, 2019; Manjula et al., 2018; Ramesh et al., 2021; Labh et al., 2019; Zafer et al., 2021; Renuka et al., 2020; Thomas et al., 2019; Valsalam et al., 2019).

2. Materials and method

2.1. Chemicals

Silver nitrate was obtained from Sigma Aldrich and Milli-Q (18.2 M Ω -cm) was attained from Cascada BIO-water Purification Scheme. The chemicals utilised in the research were all of analytic grade.

2.2. Sample group and processing of leaf extract

The leaf extracts were properly cleaned to eliminate dirt and fungal-based spores, and then shade desiccated to eliminate humidity. About 10 g of sample leaves were placed in a 250 mL beaker with 200 mL distilled water and cooked on the heating mantle for 45 min. The extract was then chilled to room temperature (T) before being sieved. This procedure was used to prepare all plant extracts (*Tabernaemontana divaricate*, *Basella alba*, and *Allium fistulosum*).

2.3. Ag NPs synthesis

For AgNPs production, a Ag nitrate solution was equipped. *Basella alba*, *Allium fistulosum*, and *Tabernaemontana divaricate* aqueous solutions are introduced in varying amounts to test tubes containing 2 mM aqueous silver nitrate solution. The studies were performed at different temperatures to find the best conditions for AgNPs production.

2.4. Characterization of synthesized Ag NPs

2.4.1. Ultraviolet-visible spectroscopy

Using a UV-visible spectrophotometer (Systronics, India Model: 2202) by a slit breadth of 2 nm and a 10 mm cell at room temperature, a UV-visible spectrophotometer by a slit breadth of 2 nm was used to analyse the extract. For proximate analysis, the material was studied in visible and UV light with wavelengths varying from 300 to 800 nm. Within an hour of starting the reaction, silver ions were reduced and silver nanoparticles were formed. AgNO₃ was used to maintain control.

2.4.2. Fourier transform infrared study

Ag NP colloid solution (50 mL) were created by ideal conditions like EFE(5%), 1 milli Molar of silver nitrate, and centrifuged at 20,000 revolutions per minute for 20 min for Fourier transform infrared (FTIR) spectroscopy measurement. The pellets were then resuspended and lyophilized for 16 h. To determine the distinctive functional groups in the produced Ag nanoparticles, FTIR analysis can be performed using Bruker, Alpha T, Germany. It gives information about a molecule's structure, which may often be gleaned from an absorption spectra.

2.4.3. X-ray powder diffraction (XRD)

Ag NP mixture was placed in a microscope glass-slide for XRD investigation. In HAO, it was dried at 50 °C. This process is repeated until a layer has been created. The dried sample was characterised employing an X-ray diffraction method (Pan Analytical, X-pert pro, Netherland) with a Cu source operated at a voltage (V) of 45 kV as well as a current (I) of 40 mA on an instrument running at a V of 45 kV and I of 40 mA.

2.4.4. Scanning electron microscope (SEM)

The shape and morphology properties of AgNPs are measured by employing a SEM. After centrifuging silver nanoparticles at 15,000 rpm for 10 mins, the pellets are collected and deposited in a dehydration oven at 50 °C to remove any remaining water. The powdered form of the Ag nanoparticle was utilized for energy dispersive XRD with a Bruker X-flash finder (Bruker, Bremen, Germany). An FEI Nova Nanolab 200 SEM was used to examine the prepared sample (FEI company Hillsboro, OR, USA). For both imaging and EDX study, the electron beam's energy was fixed at 15 keV.

2.4.5. Transmission electron Microscopy (TEM)

TEM is employed to examine the morphological characteristics of the synthesized NPs (TEM). One drop of materials was kept on a

Cu grid for TEM investigation, and then dried by employing the dry vacuum. This instrument (Tecnaï G-10, Philips) was also used to image the dried nanoemulsion, as well as an 80 kV TEM by a W-sourcing as well as an ultrahigh-resolution pole piece by 1.9 resolution.

2.5. Antioxidant reaction

The 1,1-diphenyl-2-picrylhydrazyl technique was employed to assess the free radical scavenging action of plant extract in water as a solvent (DPPH). The chemical was produced as a stock solution by a concentration of 10 mg per ml. At equal volumes, diverse concentrations of extract (200, 400, 600, 800, 1000 g) of specimen was introduced to a methanolic DPPH solution (0.1 mM). The DPPH free radical scavenging action was tested using the method elaborated by (Pan et al., 2018; Choi et al., 2017). The mixture was briskly agitated and permitted to settle at room T for 30 mins. The absorbance at 518 nm of DPPH was evaluated by employing a UV-spectrometry to assess decolorization (LMSP-UV1000B). Instead of plant extract/ascorbic acid, 0.1 mL of the appropriate vehicle was used as a control. By likening the absorbant values of control as well as an extract/compound, the % suppression of DPPH radicals by the extract/compound was calculated.

$$\text{Scavenging activity \%} = \frac{A(\text{control}) - A(\text{sample})}{A(\text{control})} \times 100$$

2.6. Antibacterial potential of synthesized silver nanoparticles

2.6.1. Bacterial culture

The microbial culture was acquired from Microbial Type Culture Collection and Gene Bank (MTCC, India). The obtained bacterial culture was confirmed using biochemical system supplied via Bergey's Manual of Systematic Bacteriology (Vol 2, Second Edition).

2.6.2. Well diffusion study

The agar-based well diffusion procedure was employed to examine the anti-microbial action of produced Ag NPs. In the petri dishes, 20 mL semi-solid mueller-hinton agar (MHA) medium was transferred. The microbes are cultivated in NB for 24 h and then cultured with 1.5 10⁶ CFU/mL suspensions of test bacteria on an exterior of solid-based medium MHA using a sterile brush (Staphylococcus aureus, Enterococcus faecalis, Escherichia coli and, Salmonella typhi). A variety of silver nanoparticle concentrations (varying from 0.32 to 10 mg/mL) were saturated onto wells by a diameter of 6 mm and kept on the surface of inoculated plates. For above 4 mentioned bacteria, petriplates were placed for 24 h at 37 °C. Ciprofloxacin is thought to be a positive control. The diameter of inhibition zone in mm was employed to quantify antimicrobial action, and all antibacterial tests are done in triplicate (Pan et al., 2018; Choi et al., 2017).

2.6.3. Antifungal activity

To test the antifungal impact of silver nanoparticles, Aspergillus niger and Candida albicans are cultured in PDA fluid media for 2 days at 35 °C, then plated on new PDA solid-based medium comprising Ag NPs and incubated for 5 days at 35 °C. Controls were Ag-free PDA plates cultivated below the similar circumstances. The colonies are measured in millimetres. Ketoconazole is utilized as a positive control in our research (Rajeshkumar and Malarkodi, 2014; Labh et al., 2019).

2.7. Anti diabetic assay

2.7.1. Alpha amylase

2.7.1.1. Procedure. The starch-iodine technique was used to measure alpha-amylase activity. 10 L of -amylase solution of 0.025 mg/mL were combined with 390 L of phosphate buffer of 0.02 M comprising 0.006 M NaCl at a pH 7.0 has various extract concentrations. After a 10-minute incubation in 37 °C, 100 L of 1% starch substance was introduced as well as the mixture was re-incubated for 1 h. The absorbance was evaluated at 565 nm after adding 0.1 mL of 1 percent iodine solution followed by 5 mL distilled H₂O. The same reaction conditions were used to determine the sample, substrate, and -amylase blank (Zafer et al., 2021). The amount of enzyme activity that was inhibited was determined as.

$$\% \text{Inhibition} = \frac{\text{Absorbance of Control} - \text{Absorbance of Sample}}{\text{Absorbance of Control}}$$

2.8. Catalytic action

2.8.1. Catalytic activity of AgNPs

The catalytic action of as-produced AgNPs for the oxidation process of benzyl alcohol was studied in order to investigate the potential use of green synthesised Ag NPs with in area of catalysis.

2.8.2. Benzyl alcohol oxidation

The catalytic performance of Ag nanoparticles produced with varying amounts (1, 5, and 10 mL) of leaf extracts as an oxidation catalyst was tested. To evaluate the reaction kinetics, the reaction mixture was obtained every 10 min and quenched instantly. The kinetics of the reaction were then analysed using gas chromatography (GC) with a capillary column. The following was the GC approach for the kinetic investigation and product analysis: The initial T of the column was 120 °C, which was then increased to 180 °C at a rate of 100 °C min⁻¹ and maintained for 10 min. The condition of the reaction was determined as well as the results were acquired using this process.

2.9. Photocatalytic action

The biologically synthesized Ag NPs were further employed for the study of dye deprivation. The reaction mixture was kept by 2 mL of eppendorf vial. Nearly 1 mL of congo red dye was added by 0.25 mg of Ag NPs. The pH was varying from 2 to 10. The aliquot parts were placed in a rotary shaker for a period of 1 hr at room T. After the incubation time the specimen was taken for centrifugation at 1000 rpm. Supernatant was taken for residual dye assessment through UV-visible spectrometer.

3. Result and discussion

3.1. Synthesis and characterization of Ag NP

Silver nanoparticle was synthesized from a biosource using three different plant extract such as *Basella alba*, *Tabernaemontana divaricata* and *Allium fistulosum*. The colour transformed from lighter brown to darker brown when the *Tabernaemontana divaricata* and *Allium fistulosum* leaf extract were introduced droplet manner to the silver nitrate mixture, indicating Ag NPs formation. Similarly, in the case of *Basella alba*, the colour variation was observed from lighter brown to green which is a property of Ag NPs. A variation in colour of the solution showed the AgNPs synthesis.

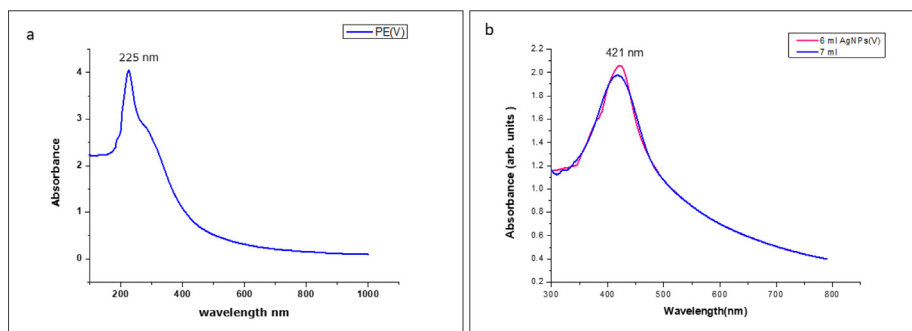


Fig. 1. (a) UV spectrum of *Allium fistulosum* leaf extract. (b) UV spectra of silver nanoparticle formulated using *Allium fistulosum* leaf extract.

The color changing of AgNO_3 mixture from colorless to darker brown signifying the NP formation that were seen via naked eye and further verified by the UV. The absorption band intensity of *Allium fistulosum* and silver nanoparticle synthesized was identified as 225 nm and 421 nm respectively in Fig. 1. The produced Ag NPs with plant extract of *Tabernaemontana divaricata*. It was observed from that the plant extract of *Tabernaemontana divaricata* and silver nanoparticles shows a extreme absorption band of 215 and 426 nm. The prominent hump specifies the creation of Ag NPs (Fig. 2).

Basella alba along with silver nanoparticles, the band intensity of produced AgNPs was identified as 223 nm and 429 nm (Fig. 3). The colour changing happened due to the surface plasmon resonance, that was an intrinsic property of metal-based NPs. There was a noteworthy improvement in peak in the Ag NPs in comparison with crude-based plant extracts (Gandhi et al., 2021; Parasuraman et al., 2019; Parasuraman et al., 2019). Generally, the UV study of Ag NPs designates a rise in the absorption band representing the more significant creation of Ag NPs. The Fig. 4 illustrates the FTIR spectra of Ag NPs produced from three diverse plant extract. The nanoparticle synthesized *Allium fistulosum* using 3 bands in the arena of $3500\text{--}1500\text{ cm}^{-1}$ with a more influential band at 1609 cm^{-1} , and a lower height at 3360 and 2114 per cm related to C=O carbonyl group, O–H stretched vibration, aromatic C–H bond in Fig. 4(a) (Anju et al., 2019; Siddhardha et al., 2020; Anand et al., 2021). The FTIR spectra of nanoparticle synthesized by *Tabernaemontana divaricata* extract revealed an absorption band at 3297 cm^{-1} ; 1634 cm^{-1} , 1347 cm^{-1} , 1324 cm^{-1} and 1065 cm^{-1} which corresponds to existence of C–H stretch, C=O bonds, C–O bonds, C–O bonds and alkylamine groups Fig. 4(b). The FTIR spectra of nanoparticle synthesized by *Basella alba* extract showed an absorption peak at 3316 , 1632 , 1372 , and 1041 cm^{-1} designates an existence of OH bond, C=C bond, S=O stretching and C–N bonds in Fig. 4(c). The Fig. 5 incitates the XRD image of Ag NPs produced from three different plant extracts. AgNPs synthesized from *Allium*

fistulosum had 2 θ ranges of 37.48° , 47.78° , 55.74° and 68.87° which corresponds to (1 1 1), (–1 1 2), (0 2 0) and (2 2 0) respectively (Fig. 5 (a)). AgNPs prepared with the extract of *Tabernaemontana divaricata*. The spectrum possesses four regions at 2θ values of 38.31° , 48.33° , 56.45° , and 69.59° relative to (1 1 1), (–2 0 2), (0 2 0) and (2 2 0) of the lattice planes of Bragg's reflection, respectively in Fig. 5(b).

The morphological nature of AgNPs are examined by employing SEM. SEM shows solid block-like structures for *Basella alba* and *Allium fistulosum* mediated AgNPs while for *Tabernaemontana divaricata* mediated AgNPs, it shows rod-like structure with some agglomeration where an average particle shape was 40, 55 and 57 nm respectively (Fig. 6 & Fig. 7).

The particle size, morphological, and crystalline were examined by employing TEM and Particle size analyser. A one drop solution of AgNPs were combined on to the carbon enclosed copper-based grid. *Basella alba*, *Tabernaemontana divaricata* and *Allium fistulosum* plant extracts were used to synthesize AgNPs and TEM images of AgNPs with dimensions of 40 nm, 55 nm and 57 nm respectively were obtained. TEM pictures showed the produced AgNPs were comparatively even in diameter and size as shown in Fig. 8 and Fig. 9 (Nithiyavathi et al., 2021; Sathiyaraj et al., 2021).

3.2. *In vitro* studies

3.2.1. Antimicrobial action of Ag NP using well diffusion technique

The antimicrobial action of Ag NP produced using plant extract was confirmed using well diffusion method, which is considered as one of the fastest and reliable method as shown in Fig. 10. The antibacterial efficiency of the silver nanoparticle is analysed with the help of microbial species like *Enterococcus faecalis*, *Escherichia coli*, *Staphylococcus aureus*, followed by *Salmonella typhi*. The sample silver nanoparticle synthesised using *Allium fistulosum*, *Tabernaemontana divaricata*, *Basella alba* is represented as V, N and P Ag. The Table 1 represents the antibacterial efficiency of silver

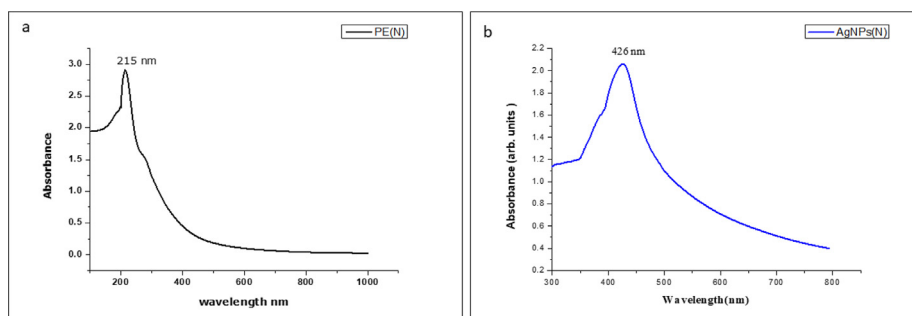


Fig. 2. (a) UV spectrum of *Tabernaemontana divaricate* leaf extract. (b) UV spectrum of silver nanoparticle formulated using *Tabernaemontana divaricate* leaf extract.

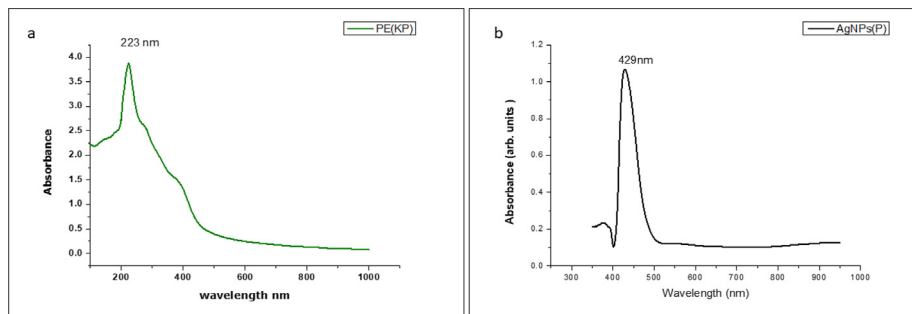


Fig. 3. (a) UV spectra of *Basella alba* leaf extract. (b) UV spectrum of Ag NP formulated using *Basella alba* leaf extract.

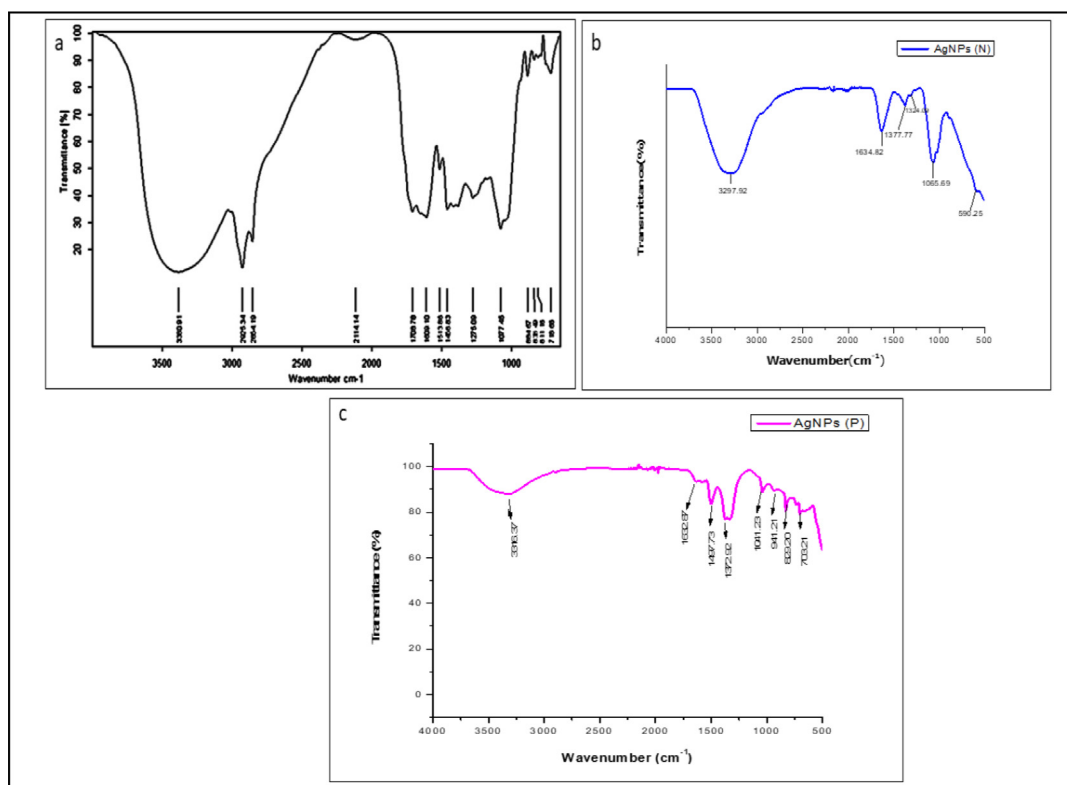


Fig. 4. (a) FTIR spectrum of produced Ag NPs from *Allium fistulosum* extract. (b) FTIR spectrum of produced Ag NPs from *Tabernaemontana divaricata* extract. (c) FTIR spectra of produced Ag NPs from *Basella alba* extract.

nanoparticle against the bacterial culture in Fig. 11. In the case of sample N(Ag), highest zone of inhibition is observed while treating with the *Salmonella typhi* then least is found with *Staphylococcus aureus* i.e. 18 mm and 08 mm respectively. Similarly, in terms of sample- P(Ag) the greatest zone of inhibition was identified while treating through *Salmonella typhi* and least was found in the case of *Escherichia coli* i.e. 17 mm and 11 mm respectively. Similarly, in the case of sample V(Ag), highest zone of inhibition is observed while treating with the *Salmonella typhi* then least is used is ciprofloxacin and its zone of inhibition is observed within a ranging from 35 to 40 mm in Fig. 12.

3.2.2. Antifungal activity of Ag NP using well diffusion method

The antifungal efficiency was studied by employing well diffusion technique towards two diverse fungal straining like *Aspergillus niger* and *Candida albicans faecalis* (Figs. 12 & 13). In the case of fungal strain, *Aspergillus niger*, the zone of inhibition followed the order V (Ag) > P (AG) > N(Ag) mediated AgNPs i.e. 11 mm,

09 mm and 08 mm respectively. Similarly, in the case of fungal strain, *Candida albicans faecalis*, the zone of inhibition followed the order V (Ag) > P (AG) > N(Ag) mediated AgNPs i.e. 10 mm, 08 mm and 07 mm respectively (Table 2).

3.2.3. Antioxidant action of produced AgNPs by employing 1,1-diphenyl-2-picrylhydrazyl (DPPH) study

The anti-oxidant action of produced AgNPs were evaluated by DPPH procedure. DPPH, steady natural free radical which was employed for examining the free radical actions and then anti-oxidant action of numerous organic substances. Different concentration of each samples such as 200, 400, 600, 800, and 1000 µg were used for the antioxidant study. *Basella alba* mediated silver nanoparticle showed higher inhibition percent at 1000 µg concentration compared to others. It also reveals that as the concentration enhances the percent suppression also enhances i.e., the percent inhibition was found to be 23–64% for the sample concentration

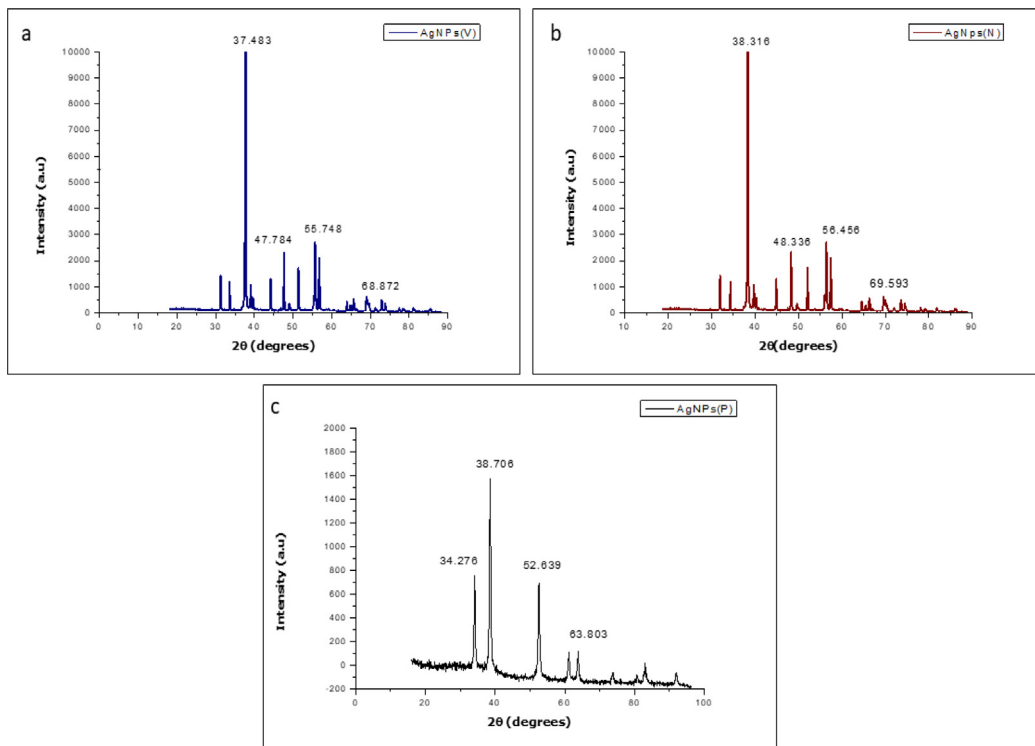


Fig. 5. (a) XRD outline of Ag NP synthesized by *Allium fistulosum* leaf extract. (b) XRD scheme of Ag NP produced by *Tabernaemontana divaricata* leaf extract. (c) XRD image of Ag NP produced by *Basella alba* leaf extract.

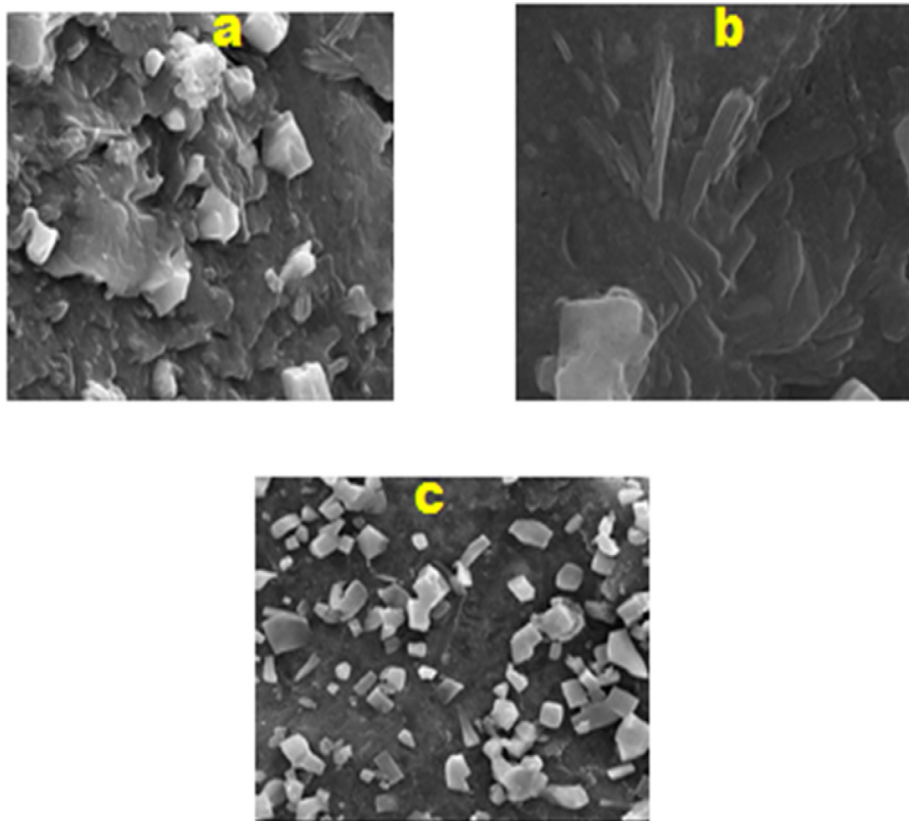


Fig. 6. (a) SEM picture of Ag NP produced through employing *Basella alba*, (b) *Tabernaemontana divaricate*, (c) *Allium fistulosum*.

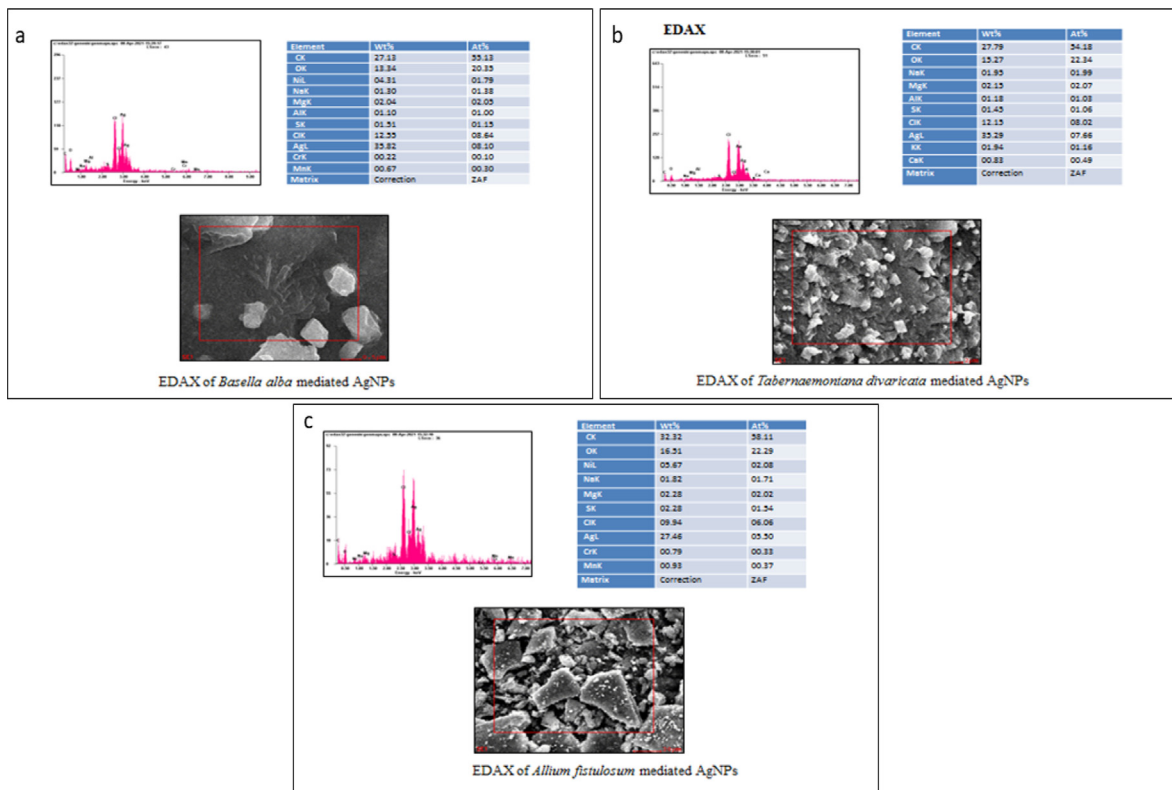


Fig. 7. EDAX analysis of *Basella alba*, *Allium fistulosum*, and *Tabernaemontana divaricata* mediated AgNPs.

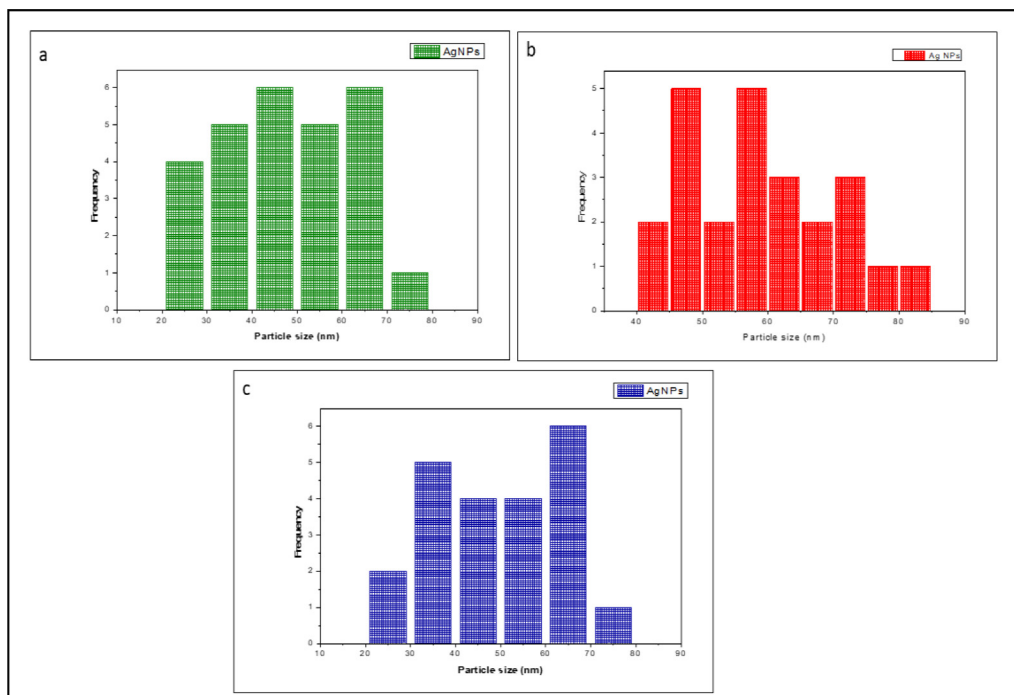


Fig. 8. Hydrodynamic size of Ag NPs produced from (a) *Basella alba*, (b) *Tabernaemontana divaricata* and (c) *Allium fistulosum* extract.

200–1000 μg (Table 3). The Fig. 14 gives a clear idea that inhibition activity is a dose dependent activity.

Similarly, both *Tabernaemontana divaricata* and *Allium fistulosum* mediated silver nanoparticle showed higher inhibition percent

at 1000 μg concentration compared to other concentrations (Tables 4 and 5). It also reveals that as the concentration enhances the percent suppression also rises i.e., the percent inhibition was found to be 34–57% and 27–46% for the sample concentration 200–1000 μg

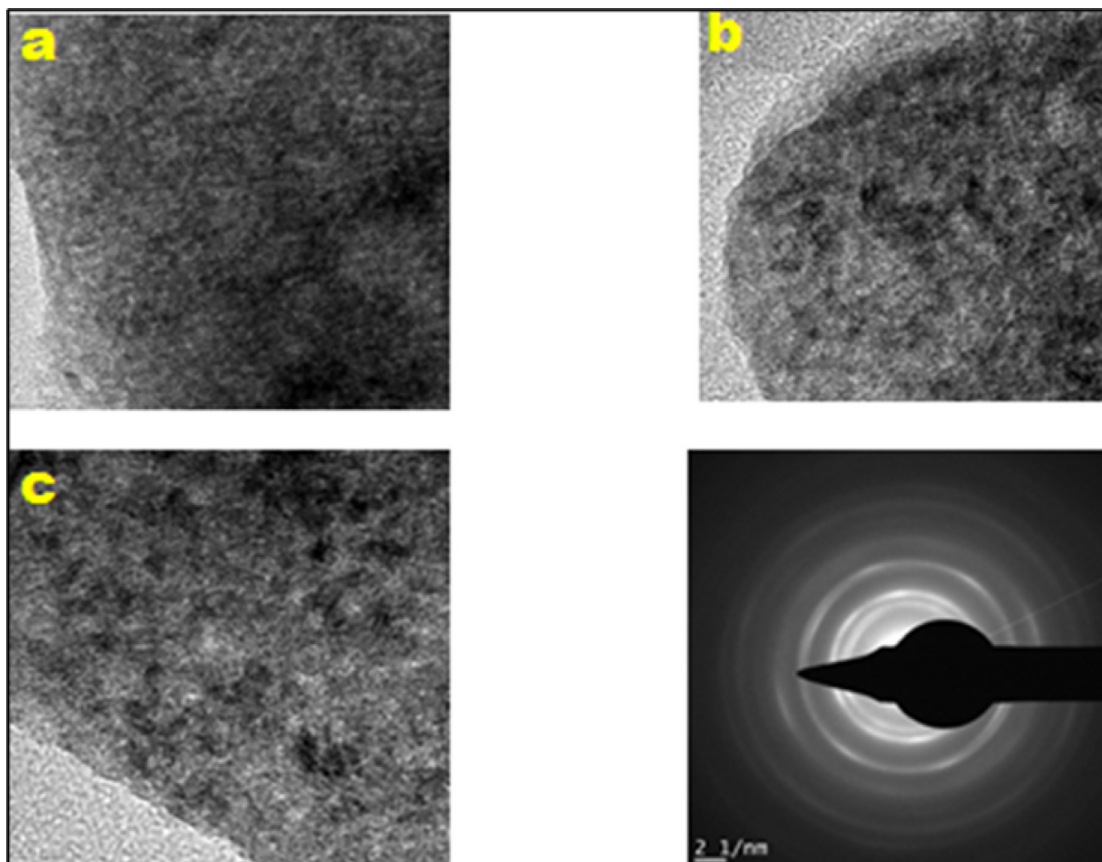


Fig. 9. TEM picture of Ag NPs synthesized from (a) *Basella alba*, (b) *Tabernaemontana divaricata* and (c) *Allium fistulosum* extract.



Fig. 10. The antibacterial effect of synthesized silver nanoparticle using (a), *Enterococcus faecalis* (b) *Staphylococcus aureus* (c) *Escherichia coli* (d) *Salmonella typhi*.

Table 1
Antibacterial efficiency of silver nanoparticles using well diffusion method.

S. No.	Microorganisms	Control	N (Ag)	P (Ag)	V (Ag)	Ciprofloxacin
1.	<i>Enterococcus faecalis</i>	-	15	13	17	35
2.	<i>Staphylococcus aureus</i>	-	08	12	10	40
3.	<i>Escherichia coli</i>	-	09	11	11	38
4.	<i>Salmonella typhi</i>	-	18	17	18	35

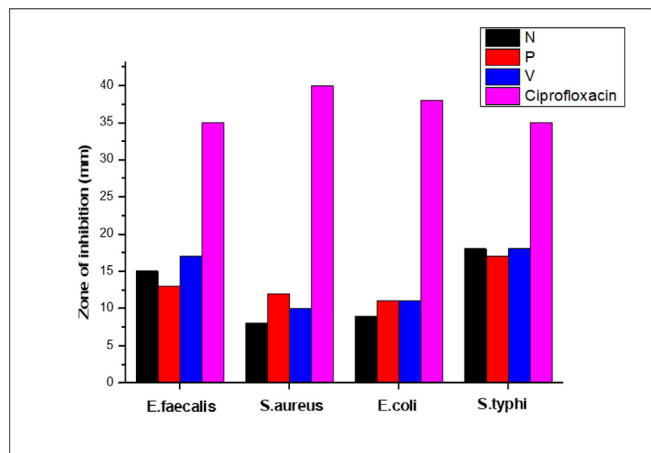


Fig. 11. The zone of inhibition revealed through Ag NP against different bacterial strains.

(Figs. 15 and 16). The reduction power of a molecule was linked to an electron transfer capability and thus might assist as a important indicator of its potent anti-oxidant action.

3.2.4. Antidiabetic action of Ag NPs synthesized by employing *Allium fistulosum*, *Tabernaemontana divaricata*, *Basella alba*

Diabetes mellitus is a set of metabolic illnesses characterised by persistently elevated blood sugar levels. Inhibiting carbohydrate digesting enzymes (-glucosidase and -amylase) is one way to treat hyperglycemia by limiting the breakdown of carbohydrates into monosaccharides, which is a major cause of high blood glucose

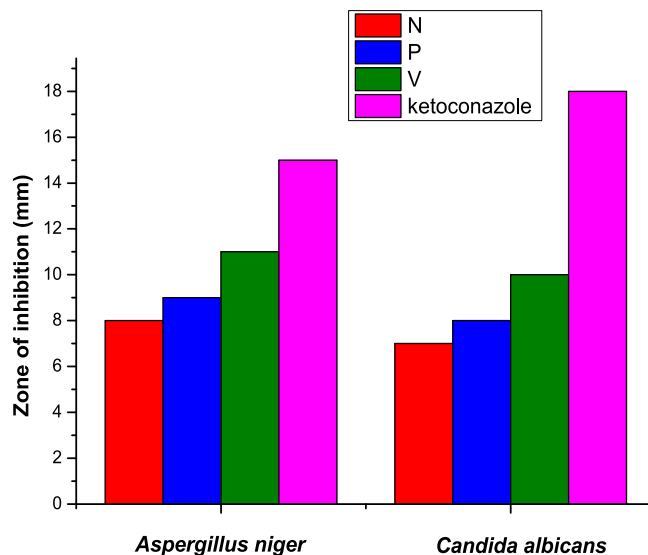


Fig. 13. The zone of inhibition exhibited by silver nanoparticle against different fungal strains.

Table 2
Antifungal efficiency of Ag NPs using well diffusion technique.

S.No.	Microorganisms	Control	N(Ag)	P(Ag)	V(Ag)	Ketoconazole
1.	<i>Aspergillus niger</i>	-	08	09	11	15
2.	<i>Candida albicans</i>	-	07	08	10	18

levels. As a result, creating drugs that inhibit carbohydrate hydrolysing enzymes could be an effective strategy to treat diabetes. The principal enzyme intricate in the interruption of polysaccharides and the proclamation of sugar into the bloodstream is alpha-amylase, that results in an increase in blood glucose levels and, eventually, diabetes. This enzyme's repressive impact may have a possible beneficial impact on diabetes. The materials were diluted into different concentrations such as 5, 10, 15, 20 and 25 g/mL in order to assess the antidiabetic property. Fig. 17 depicts the percent inhibitory impact of Ag NP on the enzyme. Ag NP showed a repressive impact on an enzyme in a dosage-based manner as well as when the dosage was enlarged to 25 µg/mL. It might be evalu-

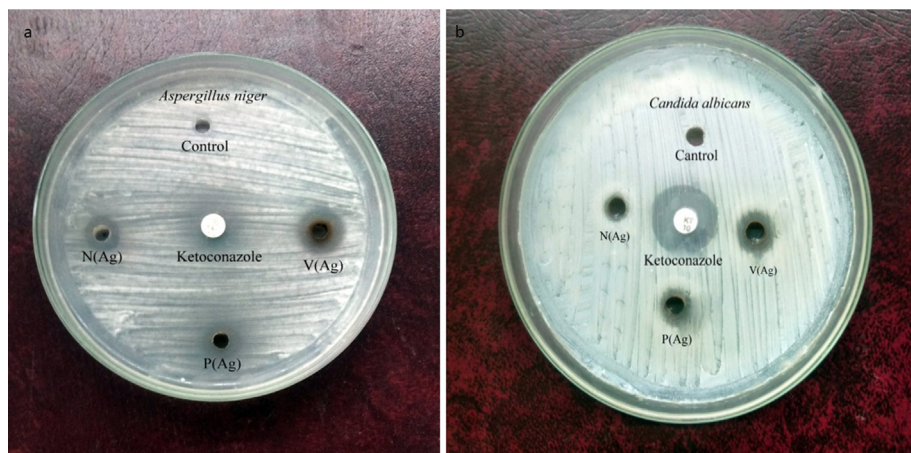


Fig. 12. The antifungal effect of synthesized silver nanoparticle using (a), *Aspergillus niger*, (b) *Candida albicans faecalis*.

Table 3
Antioxidant activity of *Basella alba* mediated Silver nanoparticle.

Concentrations (µg)	Percentage inhibition AgNPs	Percentage inhibition Control
200	23	81.34
400	33.52	89.65
600	45.97	91.76
800	53.56	95.48
1000	64.85	95.17

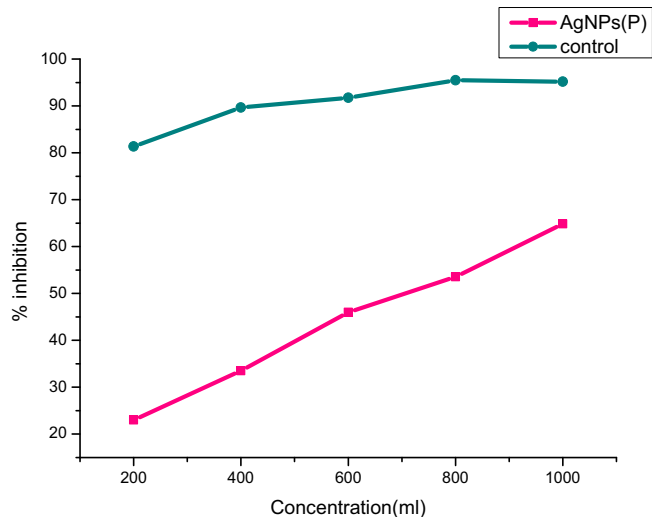


Fig. 14. Percentage inhibition of silver nanoparticle synthesized using *Basella alba*.

Table 4
Antioxidant activity of *Tabernaemontana divaricate* mediated Silver nanoparticle.

Concentrations (µg)	Percentage inhibition AgNPs	Percentage inhibition Control
200	34.35	75.54
400	38.45	83.85
600	43.46	85.82
800	53.18	92.42
1000	57.53	97.15

Table 5
Antioxidant activity of *Allium fistulosum* mediated Silver nanoparticle.

Concentrations (µg)	Percentage inhibition AgNPs	Percentage inhibition Control
200	27.13	79.14
400	31.15	83.47
600	35.48	88.69
800	41.24	91.51
1000	46.79	95.28

ated from the outcomes that Ag NP might act as a substitute due to its potent repressive impact which have on its enzyme. The result also suggests that silver nanoparticle synthesized using *Tabernaemontana divaricata* showed higher inhibition compared to the silver prepared from other two source such as *Basella alba* and *Allium fistulosum*. Around 80% of inhibition was found in silver nanoparticle synthesized by *Tabernaemontana divaricata* at the concentration of 25 µg/mL.

3.2.5. Catalytic action

The catalytic action of three different extracts of AgNPs were shown in Fig. 18 which was found as 60, 100 and 100 mins for

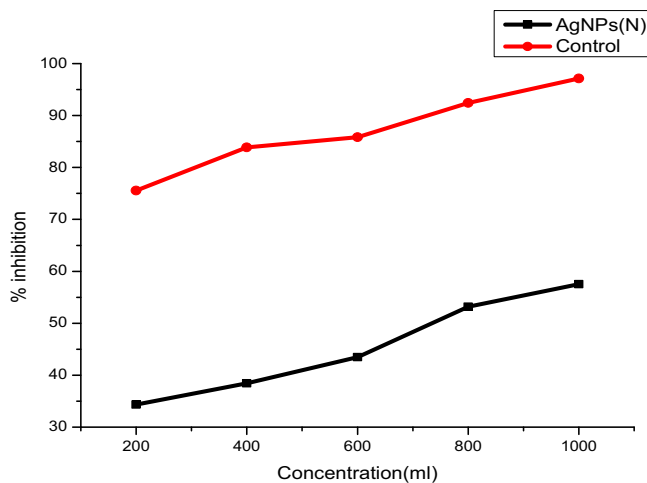


Fig. 15. Percentage inhibition of silver nanoparticle synthesized using *Tabernaemontana divaricata*.

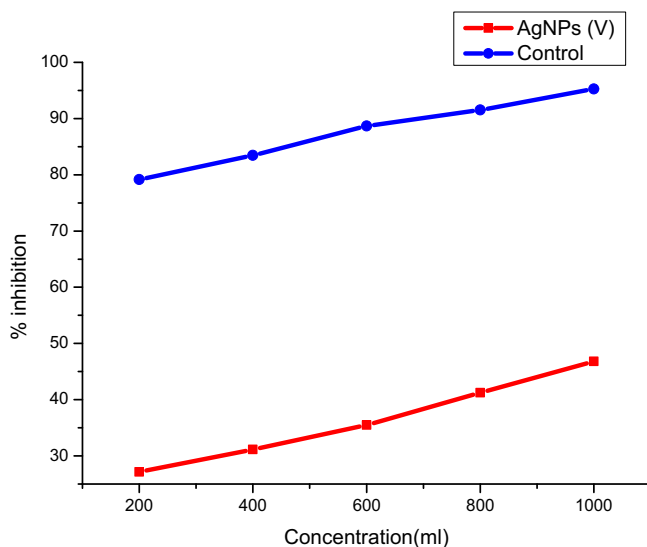


Fig. 16. Percentage inhibition of Ag NP synthesized utilizing *Allium fistulosum*.

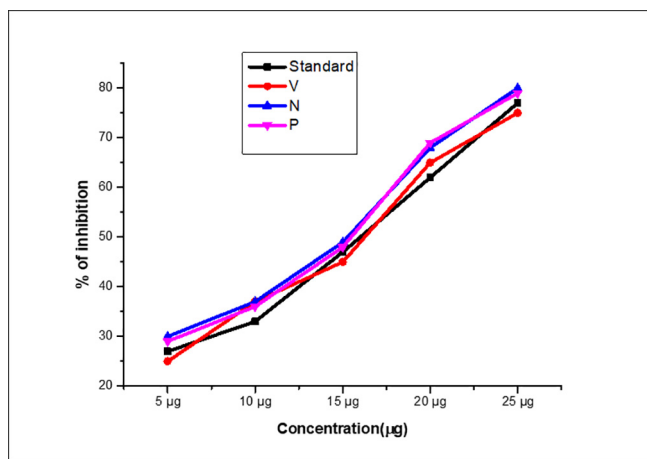


Fig. 17. Anti-diabetic activity of silver nanoparticle (Alpha-amylase).

Tabernaemontana divaricate (N), *Allium fistulosum* (V) and *Basella alba* (P) respectively. When the AgNPs were pre-processed by employing the 1 mL plant extract (V), the conversion by-product

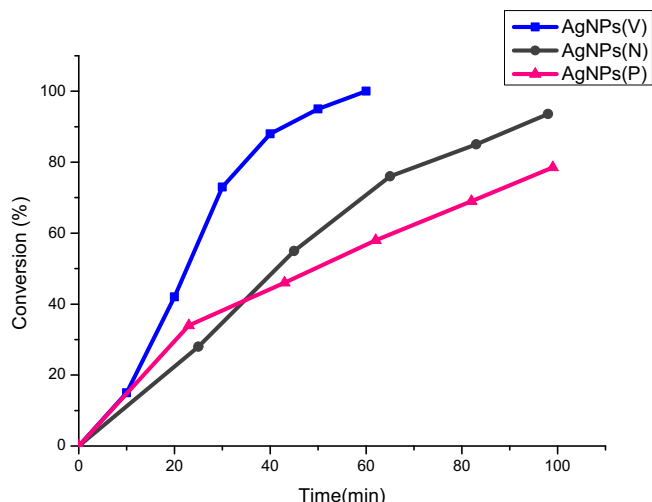


Fig. 18. Catalytic activity of Ag NPs.

creation starts 10 min once the reaction get initiated and gradually proceeds against 100% conversion product that is benzaldehyde was attained after 50 min of reaction period. Nevertheless, when Ag NPs were made with 5 mL plant extract (N), the reaction kinetics were discovered to be differ from the formerly used method (V). The reaction begins with a conversion of 65 percent after 20 min, but it is terminated after 100 min, providing a maximum conversion of 93.6 percent, which is quite different from the previous catalyst, which yielded a 100 percent conversion product in 50 min (Vinayagam et al., 2022; Magdalane et al., 2021; Subbareddy et al., 2020; Thirupathy et al., 2020). Likewise, the catalytic performance of Ag NPs ready with 10 mL plant extract (P) was assessed. It was discovered that 20 min at the beginning of the reaction, 34% of the conversion product was developed, whilst at the end of 100 min, a maximum of 78.5 percent conversion product was procured, as well as the reaction was not proceeded further. Based on the foregoing findings, it can be concluded that the Ag nanoparticles made with 1 mL plant extract were of good quality produced a 100 per cent conversion product in 50 min of reaction period.

3.2.6. Photocatalytic action

Figure shows the photocatalytic action of all the 3 extracts at various time and concentration. The optimized Ag NP was taken for the application of dye degradation process by varying the con-

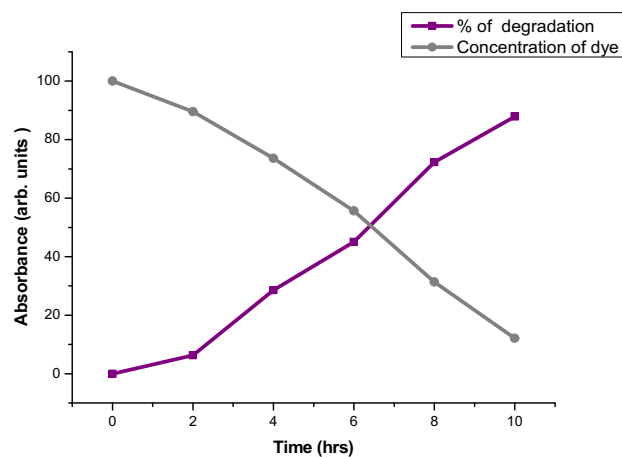
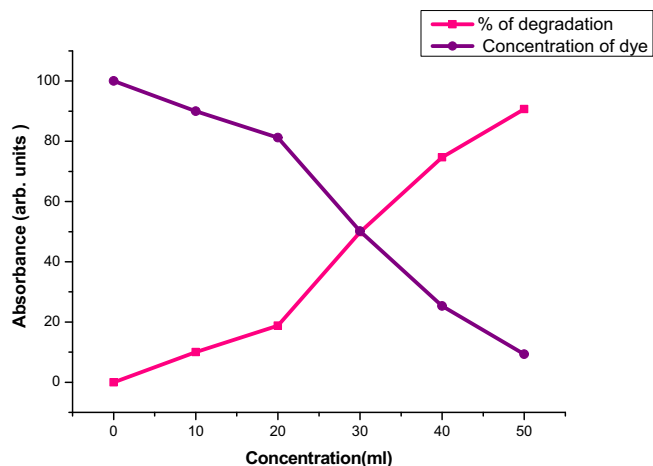


Fig. 20. Catalytic activity of Ag NPs with Allium fistulosum.

centration from 0 to 50 of different aliquots of Ag NPs dispersions at different time of 0 to 10 and about 1 mL of congo red (1×10^{-4} M) was mixed with 0.25 mg of Ag NPs and kept for continuous stirring at room temperature. The absorbance of the reaction was observed and it was exemplified in Figs. 19–21. The clear surface plasmon resonance (SPR) band for dye was observed in 433 nm. At pH 6 SPR band in 433 has been disappeared (Geetha et al., 2018; Badineni et al., 2021).

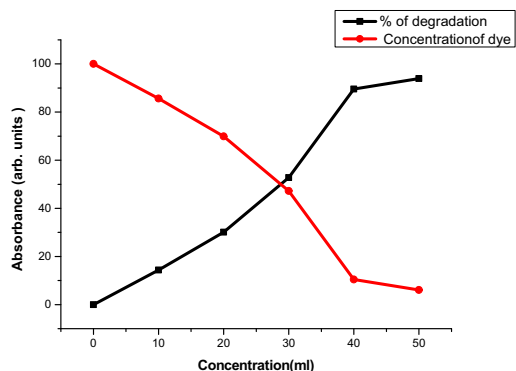
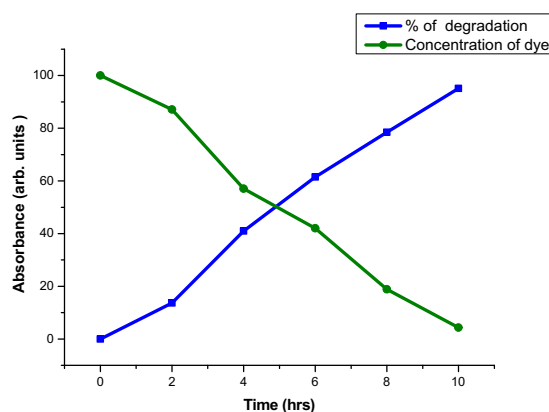


Fig. 19. Catalytic activity of Ag NPs with Tabernaemontana divaricate.



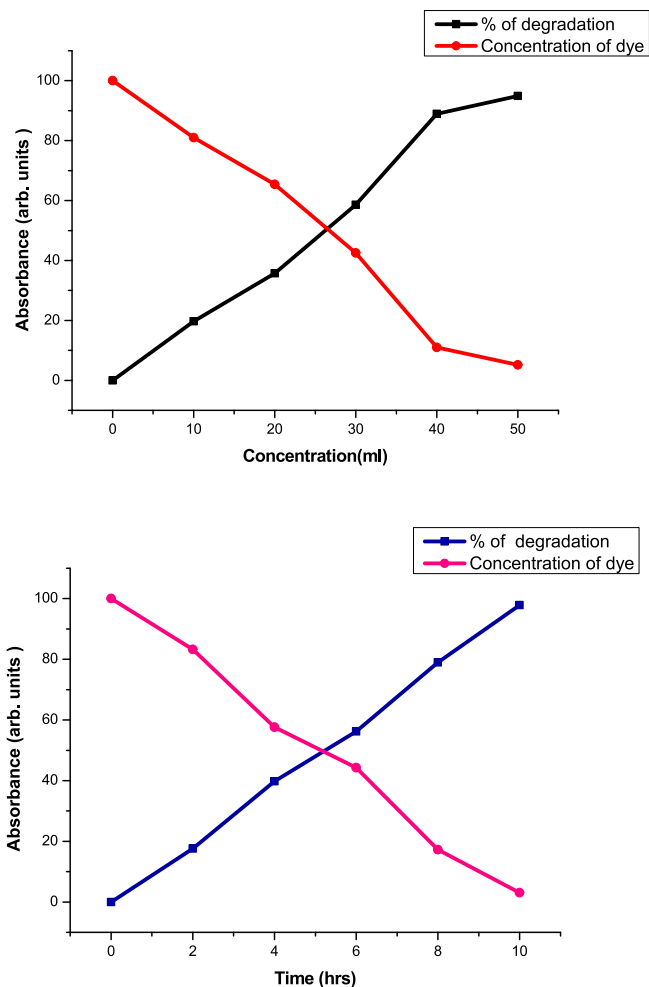


Fig. 21. Catalytic activity of Ag NPs with *Basella alba*.

4. Conclusion

Plant extracts such as *Allium fistulosum*, *Tabernaemontana divaricata*, and *Basella alba* have been successfully used to synthesise silver nanoparticles in a lesser price, eco-friendly approach. UV, FTIR, XRD, TEM and SEM were used to characterise the synthesised silver nanoparticles. Biosynthesised AgNPs are nontoxic and have antibacterial, antifungal, antioxidant, and anti-diabetic properties. Silver nanoparticles synthesised with *Allium fistulosum* (V-Ag) demonstrated a good zone of inhibition against both bacterial and fungal strains among the three sources of synthesis. When it comes to antioxidants and antidiabetics, research demonstrate that as concentration rises, so does action. The findings are highly positive, demonstrating a significant increase in the activity of the undamaged fractions. The use of biological sources to synthesise nanoparticles adds a new dimension to all application areas.

Conflict of interest

All the authors of this manuscript have no conflicts.

References

Ahmad, S., Munir, S., Zeb, N., Ullah, A., Khan, B., Ali, J., Bilal, M., Omer, M., Alamzeb, M., Salman, S.M., Ali, S., 2019. Green nanotechnology: A review on green synthesis of silver nanoparticles—An ecofriendly approach. *Int. J. Nanomed.* 14, 5087.

Akintelu, S.A., Folorunso, A.S., 2019. Characterization and antimicrobial investigation of synthesized silver nanoparticles from *Annona muricata* leaf extracts. *J. Nanotechnol. Nanomed. Nanobiotechnol.* 6, 1–5.

N.M.I. Alhaji, D. Nathiya, K. Kaviyarasu, M. Meshram, A. Ayeshamariam, A comparative study of structural and photocatalytic mechanism of AgGaO₂ nanocomposites for equilibrium and kinetics evaluation of adsorption parameters, *Surfaces Interfaces* 17, 100375, 2019.

A.M. Amanulla, C.M. Magdalane, S. Saranya, R. Sundaram, K. Kaviyarasu, Selectivity, stability and reproducibility effect of CeM-CeO₂ modified PIGE electrode for photoelectrochemical behaviour of energy application, *Surfaces and Interfaces* 22, 100835, 2021.

Anand, K., Kaviyarasu, K., Muniyasamy, S., Roopan, S.M., Gengan, R.M., Chuturgoon, A.A., 2017. Bio-synthesis of silver nanoparticles using agroforestry residue and their catalytic degradation for sustainable waste management. *J. Cluster Sci.* 28 (4), 2279–2291.

Anand, G.T., Sundaram, S.J., Kanimozhi, K., Nithiyavathi, R., Kaviyarasu, K., 2021. Microwave assisted green synthesis of CuO nanoparticles for environmental applications. *Mater. Today: Proc.* 36, 427–434.

Anju, V.T., Paramanatham, P., Sruthil Lal, S.B., Sharan, A., Syed, A., Bahkali, N.A., Alsaedi, M.H., Kaviyarasu, K., Busi, S., 2019. Antimicrobial photodynamic activity of toluidine blue-carbon nanotube conjugate against *Pseudomonas aeruginosa* and *Staphylococcus aureus*-understanding the mechanism of action. *Photodiagn. Photodyn. Ther.* 27, 305–316.

Aziz, N., Pandey, R., Barman, I., Prasad, R., 2016. Leveraging the attributes of mucor hiemalis-derived silver nanoparticles for a synergistic broad-spectrum antimicrobial platform. *Front. Microbiol.* 7, 1984. <https://doi.org/10.3389/fmicb.2016.01984>.

Badineni, V., Maseed, H., Arla, S.K., Subbareddy Yerramala, B., Naidu, V.K., Kaviyarasu, K., 2021. Effect of PVA/PVP protective agent on the formation of silver nanoparticles and its photocatalytic and antimicrobial activity. *Mater. Today: Proc.* 36, 121–125.

Bakht Dalir, S.J., Djahaniani, H., Nabati, F., Hekmati, M., 2020. Characterization and the evaluation of antimicrobial activities of silver nanoparticles biosynthesized from *Carya illinoensis* leaf extract. *Heliyon* 6, (3) e03624.

Chang, T.C., Jang, H.D., Lin, W.D., Duan, P.F., 2016. Antioxidant and antimicrobial activities of commercial rice wine extracts of Taiwanese *Allium fistulosum*. *Food Chem.* 190, 724–729.

Choi, H.K., Hwang, J.T., Nam, T.G., Kim, S.H., Min, D.K., Park, S.W., Chung, M.Y., 2017. Welsh onion extract inhibits PCSK9 expression contributing to the maintenance of the LDLR level under lipid depletion conditions of HepG2 cells. *Food Funct.* 8 (12), 4582–4591.

Dhand, V., Soumya, L., Bharadwaj, S., Chakra, S., Bhatt, D., Sreedhar, B., 2016. Green synthesis of silver nanoparticles using *Coffea arabica* seed extract and its antibacterial activity. *Mater. Sci. Eng. C. Mater. Biol. Appl.* 58, 36–43.

Elbeshehy, E.K.F., Elazzazy, A.M., Aggelis, G., 2015. Silver nanoparticlessynthesis mediated by new isolates of *Bacillus* spp., nanoparticle characterization and their activity against bean yellow mosaic virus and human pathogens. *Front. Microbiol.* 6 (453).

Arumugam Dhanesh Gandhi, K Kaviyarasu, Nookala Supraja, Rajendran Velmurugan, Gunasekaran Suriyakala, Ranganathan Babujanathanam, Yang Zang, Khantong Soontarapa, Khalid S Almaary, Mohamed S Elshikh, Tse-Wei Chen, Annealing dependent synthesis of cyto-compatible nano-silver/calcium hydroxyapatite composite for antimicrobial activities, *Arabian Journal of Chemistry* 14 (11), 103404, 2021.

Geetha, N., Sivaranjani, S., Ayeshamariam, A., Siva Bharathy, M., Nivetha, S., Kaviyarasu, K., Jayachandran, M., 2018. High performance photo-catalyst based on nanosized ZnO-TiO₂ nanoplatelets for removal of RhB under visible light irradiation. *J. Adv. Microsc. Res.* 13 (1), 12–19.

George, A., Magimai Antoni Raj, D., Venci, X., Dhayal Raj, A., Albert Irudayaraj, A., Josephine, R.L., John Sundaram, S., Al-Mohaimed, A.M., Al Farraj, D.A., Chen, T.-W., Kaviyarasu, K., 2022. Photocatalytic effect of CuO nanoparticles flower-like 3D nanostructures under visible light irradiation with the degradation of methylene blue (MB) dye for environmental application. *Environ. Res.* 203, 111880.

Kalaimagal, C., 2019. In vitro antioxidant activity in ethanolic leaf extract of *Tabernaemontana divaricata* (L.). *International Journal of Bio-Pharma Research* 8 (6), 2602–2606.

Kasinathan, K., Kennedy, J., Elayaperumal, M., Henini, M., Malik, M., 2016. Photodegradation of organic pollutants RhB dye using UV simulated sunlight on ceria based TiO₂ nanomaterials for antibacterial applications. *Sci. Rep.* 6 (1), 1–12.

Kayalvizhi, K., Alhaji, N.M.I., Saravanakumar, D., Mohamed, S.B., Kaviyarasu, K., Ayeshamariam, A., Al-Mohaimed, A.M., AbdelGawwad, M.R., Elshikh, M.S., 2022. Adsorption of copper and nickel by using sawdust chitosan nanocomposite beads – A kinetic and thermodynamic study. *Environ. Res.* 203, 111814.

Labh, A.K., Rajeshkumar, S., Roy, A., Santhoshkumar, J., Lakshmi, T., 2019. Herbal formulation mediated synthesis of silver nanoparticles and its antifungal activity against *Candida albicans*. *Indian J. Public Health Res. Dev.* 10 (11), 3454.

Loo, Y.Y., Rukayadi, Y., Nor-Khaizura, M.A.R., Kuan, C.H., Chieng, B.W., Nishibuchi, M., Radu, S., 2018. In vitro antimicrobial activity of green synthesized silver nanoparticles against selected gram-negative foodborne pathogens. *Front. Microbiol.* 9, 1555.

Magdalane, C.M., Priyadharsini, G.M.A., Kaviyarasu, K., Jothi, A.I., Simiyon, G.G., 2021. Synthesis and characterization of TiO₂ doped cobalt ferrite nanoparticles

- via microwave method: investigation of photocatalytic performance of congo red degradation dye. *Surfaces Interfaces* 25.
- Mahmoud, W.M., Abdelmoneim, T.S., Elazzazy, A.M., 2016. The impact of silver nanoparticles produced by *Bacillus pumilus* as antimicrobial and nematocide. *Front. Microbiol.* 7, 1746. <https://doi.org/10.3389/fmicb.2016.01746>.
- S. Mangala Nagasundari K. Muthu K. Kaviyarasu D.A.A. Farraj R.M. Alkufeidy Current trends of Silver doped Zinc oxide nanowires photocatalytic degradation for energy and environmental application *Surfaces and Interfaces* 23 2021 100931 100931.
- M. Mani R. Harikrishnan P. Purushothaman S. Pavithra P. Rajkumar S. Kumaresan D. A. Al Farraj M.S. Elshikh B. Balasubramanian K. Kaviyarasu Systematic green synthesis of silver oxide nanoparticles for antimicrobial activity *Environmental Research* 202 2021 111627 111627.
- M. Mani, Mohammad K. Okla, S. Selvaraj, A. Ram Kumar, S. Kumaresan, Azhaguchamy Muthukumar, K. Kaviyarasu, Mohamed A. El-Tayeb, Yahya B. Elbadawi, Khalid S. Almaary, Bander Mohsen Ahmed Almunqedi, Mohamed Soliman Elshikh, A novel biogenic *Allium cepa* leaf mediated silver nanoparticles for antimicrobial, antioxidant, and anticancer effects on MCF-7 cell line, *Environmental Research*, 198, 2021, 111199.
- Mani, M., Pavithra, S., Mohanraj, K., Kumaresan, S., Alotaibi, S.S., Eraqi, M.M., Gandhi, A.D., Babujanarthanam, R., Maaza, M., Kaviyarasu, K., 2021. Studies on the spectrometric analysis of metallic silver nanoparticles (Ag NPs) using *Basella alba* leaf for the antibacterial activities. *Environ. Res.* 199, 111274.
- Manikandan, R., Beulaja, M., Thiagarajan, R., Palanisamy, S., Goutham, G., Koodalingam, A., Prabhu, N.M., Kannapiran, E., Basu, M.J., Arulvasu, C., Arumugam, M., 2017. Biosynthesis of silver nanoparticles using aqueous extract of *Phyllanthus acidus* L. fruits and characterization of its antiinflammatory effect against L202exposed rat peritoneal macrophages. *Proc. Biochem.* 55, 172–181.
- Manjula, N., Selvan, G., Hameedha Beevi, A., Kaviyarasu, K., Ayeshamariam, A., Punnithavelan, N., Jayachandran, M., 2018. Feasibility studies on avocado as reducing agent in TiO₂ doped with Ag₂O and Cu₂O nanoparticles for biological applications. *J. Bionanosci.* 12 (5), 652–659.
- Maria Magdalane, C., Kaviyarasu, K., Raja, A., Arularasu, M.V., Mola, G.T., Isaev, A.B., Al-Dhabi, N.A., Arasu, M.V., Jeyaraj, B., Kennedy, J., Maaza, M., 2018. Photocatalytic decomposition effect of erbium doped cerium oxide nanostructures driven by visible light irradiation: Investigation of cytotoxicity, antibacterial growth inhibition using catalyst. *J. Photochem. Photobiol.* B 185, 275–282.
- Masum, M., Islam, M., Siddiqi, M., Ali, K.A., Zhang, Y., Abdallah, Y., Ibrahim, E., Qiu, W., Yan, C., Li, B., 2019. Biogenic synthesis of silver nanoparticles using *Phyllanthus emblica* fruit extract and its inhibitory action against the pathogen *Acidovorax oryzae* strain RS-2 of rice bacterial brown stripe. *Front. Microbiol.* 10, 820.
- Nakhjavani, M., Nikkha, V., Sarafraz, M.M., Shoja, S., Sarafraz, M., 2017. Green synthesis of silver nanoparticles using green tea leaves: experimental study on the morphological, rheological and antibacterial behaviour. *Heat Mass Transfer* 53 (10), 3201–3209.
- Nithiyavathi, R., John Sundaram, S., Theophil Anand, G., Raj Kumar, D., Dhayal Raj, A., Al, D.A., Farraj, R.M., Aljowaie, M.R., AbdelGawwad, Y., Samson, K.K., 2021. Gum mediated synthesis and characterization of CuO nanoparticles towards infectious disease-causing antimicrobial resistance microbial pathogens. *J. Infect. Public Health* 14 (12), 1893–1902.
- Oves, M., Aslam, M., Rauf, M.A., Qayyum, S., Qari, H.A., Khan, M.S., Alam, M.Z., Tabrez, S., Pugazhendhi, A., Ismail, I.M.I., 2018. Antimicrobial and anticancer activities of silver nanoparticles synthesized from the root hair extract of *Phoenix dactylifera*. *Mater. Sci. Eng. C Mater. Biol. Appl.* 89, 429–443.
- Pan, Y., Zheng, Y.M., Ho, W.S., 2018. Effect of quercetin glucosides from *Allium* extracts on HepG2, PC-3 and HT-29 cancer cell lines. *Oncol. Lett.* 15 (4), 4657–4661.
- Panimalar, S., Logambal, S., Thambidurai, R., Imozhi, C., Uthrakumar, R., Muthukumar, A., Rasheed, R.A., Gatashah, M.K., Raja, A., Kennedy, J., Kaviyarasu, K., 2022. Effect of Ag doped MnO₂ nanostructures suitable for wastewater treatment and other environmental pollutant applications. *Environ. Res.* 205, 112560.
- Panimalar, S., Subash, M., Chandrasekar, M., Uthrakumar, R., Imozhi, C., Al-Onazi, W.A., Al-Mohaimed, A.M., Chen, T.-W., Kennedy, J., Maaza, M., Kaviyarasu, K., 2022. Reproducibility and long-term stability of Sn doped MnO₂ nanostructures: Practical photocatalytic systems and wastewater treatment applications. *Chemosphere* 293, 133646.
- Parasuraman, P., Anju, V.T., Sruthil Lal, S.B., Sharan, A., Busi, S., Kaviyarasu, K., Arshad, M., Dawoud, T.M.S., Syed, A., 2019. Synthesis and antimicrobial photodynamic effect of methylene blue conjugated carbon nanotubes on *E. coli* and *S. aureus*. *Photochem. Photobiol. Sci.* 18 (2), 563–576.
- Parasuraman, P., Antony, A.P., B. S.L.S., Sharan, A., Siddhardha, B., Kasinathan, K., Bahkali, N.A., Dawoud, T.M.S., Syed, A., Antony, Asha P., 2019. Antimicrobial photodynamic activity of toluidine blue encapsulated in mesoporous silica nanoparticles against *Pseudomonas aeruginosa* and *Staphylococcus aureus*. *Biofouling* 35 (1), 89–103.
- Perumal, V., Imozhi, C., Uthrakumar, R., Robert, R., Chandrasekar, M., Mohamed, S. B., Honey, S., Raja, A., Al-Mekhlafi, F.A., Kaviyarasu, K., 2022. Enhancing the photocatalytic performance of surface - Treated SnO₂ hierarchical nanorods against methylene blue dye under solar irradiation and biological degradation. *Environ. Res.* 209, 112821.
- Rafique, M., Sadaf, I., Rafique, M.S., Tahir, M.B., 2017. A review on green synthesis of silver nanoparticles and their applications. *Artif. Cells Nanomed. Biotechnol.* 45 (7), 1272–1291.
- Rai, M., Kon, K., Ingle, A., Duran, N., Galdiero, S., Galdiero, M., 2014. Broad-spectrum bioactivities of silver nanoparticles: the emerging trends and future prospects. *Appl. Microbiol. Biotechnol.* 98 (5), 1951–1961.
- Rajeshkumar, S., Malarkodi, C., 2014. In Vitro Antibacterial Activity and Mechanism of Silver Nanoparticles against Foodborne Pathogens. *Bioinorg. Chem. Appl.* 2014, 1–10.
- Ramesh, R., Yamini, V., Sundaram, S.J., Khan, F.L.A., Kaviyarasu, K., 2021. Investigation of structural and optical properties of NiO nanoparticles mediated by *Plectranthus amboinicus* leaf extract. *Mater. Today: Proc.* 36, 268–272.
- Renuka, R., Renuka Devi, K., Sivakami, M., Thilagavathi, T., Uthrakumar, R., Kaviyarasu, K., 2020. Biosynthesis of silver nanoparticles using *Phyllanthus emblica* fruit extract for antimicrobial application. *Biocatalysis and Agric. Biotechnol.* 24.
- Sanchooli, N., Saeidi, S., Barani, H.K., Sanchooli, E., 2018. In vitro antibacterial effects of silver nanoparticles synthesized using *Verbena officinalis* leaf extract on *Yersinia ruckeri*, *Vibrio cholera* and *Listeria monocytogenes*. *Iranian journal of microbiology* 10 (6), 400.
- Sathiyaraj, S., Suriyakala, G., Dhanesh Gandhi, A., Babujanarthanam, R., Almaary, K. S., Chen, T.-W., Kaviyarasu, K., 2021. Biosynthesis, characterization, and antibacterial activity of gold nanoparticles. *J. Infect. Public Health* 14 (12), 1842–1847.
- Siddhardha, Busi, Pandey, Uday, Kaviyarasu, K., Pala, Rajasekharreddy, Syed, Asad, Bahkali, Ali H., Elgorban, Abdallah M., 2020. Chrysin-loaded chitosan nanoparticles potentiates antibiofilm activity against *Staphylococcus aureus*. *Pathogens* 9 (2), 115.
- Simbine, E.O., Rodrigues, L.D.C., Lapa-Guimaraes, J., Kamimura, E.S., Corassin, C.H., Oliveira, C.A.F.D., 2019. Application of silver nanoparticles in food packages: a review. *Food Sci. Technol.* 39 (4), 793–802.
- Y. Subbareddy, R. Naresh Kumar, B.K. Sudhakar, K. Rayappa Reddy, Surendra Kumar Marth, K. Kaviyarasu, A facile approach of adsorption of acid blue 9 on aluminium silicate-coated Fuller's Earth - Equilibrium and kinetics studies, *Surfaces Interfaces* 19, 100503, 2020.
- Syafuiddin, A., Salmiati, Salim, M.R., Beng Hong Kueh, A., Hadibarata, T., Nur, H., 2017. A review of silver nanoparticles: research trends, global consumption, synthesis, properties, and future challenges. *J. Chin. Chem. Soc.* 64 (7), 732–756.
- Thirupathy, C., Lims, S.C., Sundaram, S.J., Mahmood, A.H., Kaviyarasu, K., 2020. Equilibrium synthesis and magnetic properties of BaFe₁₂O₁₉/NiFe₂O₄ nanocomposite prepared by co precipitation method. *J. King Saud Univ.-Sci.* 32 (2), 1612–1618.
- Thomas, B., Vithiya, B.S.M., Prasad, T.A.A., Mohamed, S.B., Magdalane, C.M., Kaviyarasu, K., Maaza, M., 2019. Antioxidant and Photocatalytic Activity of Aqueous Leaf Extract Mediated Green Synthesis of Silver Nanoparticles Using *Passiflora edulis* f. *flavicarpa*. *J. Nanosci. Nanotechnol.* 19 (5), 2640–2648.
- Tippayawat, P., Phromviyo, N., Boueroy, P., Chompoosor, A., 2016. Greensynthesis of silver nanoparticles in Aloe vera plant extract prepared by a hydrothermal method and their synergistic antibacterial activity. *PeerJ* 4, e2589.
- Tippayawat, P., Phromviyo, N., Boueroy, P., Chompoosor, A., 2016. Green synthesis of silver nanoparticles in Aloe vera plant extract prepared by a hydrothermal method and their synergistic antibacterial activity. *PeerJ* 4, e2589.
- Valsalam, S., Agastian, P., Arasu, M.V., Al-Dhabi, N.A., Ghilan, A.-K., Kaviyarasu, K., Ravindran, B., Chang, S.W., Arokiyaraj, S., 2019. Rapid biosynthesis and characterization of silver nanoparticles from the leaf extract of *Tropaeolum majus* L. and its enhanced in-vitro antibacterial, antifungal, antioxidant and anticancer properties. *J. Photochem. Photobiol.* B 191, 65–74.
- Venkatesh, N., Bhowmik, H., Kula, A., 2018. Metallic nanoparticle: a review. *Biochemical Journal of Scientific & Technical Research* 4 (2), 3765–3775.
- Ramesh Vinayagam, Yash Patnaik, P Brijesh, Deepa Prabhu, Melisha Quadras, Shraddha Pai, Manoj Kumar Narasimhan, K. Kaviyarasu, Thivaharan Varadavenkatesan, Raja Selvaraj, Superparamagnetic hematite spheroids synthesis, characterization, and catalytic activity, *Chemosphere*, 294, 2022, 133730.
- Yadi, M., Mostafavi, E., Saleh, B., Davaran, S., Aliyeva, I., Khalilov, R., Nikzamid, M., Nikzamid, N., Akbarzadeh, A., Panahi, Y., Milani, M., 2018. Current developments in green synthesis of metallic nanoparticles using plant extracts: a review. *Artif. Cells Nanomed. Biotechnol.* 46 (sup3), S336–S343.
- Yaqoob, A.A., Umar, K., Ibrahim, M.N.M., 2020. Silver nanoparticles: various methods of synthesis, size affecting factors and their potential applications—a review. *Applied Nanoscience* 10 (5), 1369–1378.
- Zafer, J.B., Dede, S., Karakuş, E., 2021. α -Amylase assay with starch-iodine-sodium fluorescein-based fluorometric method in human serum samples. *Prep. Biochem. Biotech.* 51 (6), 599–606.
- Zhao, C., Wang, Z., Cui, R., Su, L., Sun, X., Borrás-Hidalgo, O., Li, K., Wei, J., Yue, Q., Zhao, L., 2021. Effects of nitrogen application on phytochemical component levels and anticancer and antioxidant activities of *Allium fistulosum*. *PeerJ* 9, e11706.
- Zuo, M., Liu, X.X., Liu, D., Zhao, H.Y., Xuan, L.L., Jiang, W.X., Li, W.Z., 2018. Extraction, characterization and antioxidant activity in vitro of proteins from *Semen Allii Fistulosi*. *Molecules* 23 (12), 3235.